

Article

# Evolution of the Beaches in the Regional Park of Salinas and Arenales of San Pedro del Pinatar (Southeast of Spain) (1899–2019)

Daniel Ibarra-Marinas, Francisco Belmonte-Serrato, Gustavo A. Ballesteros-Pelegrín \*   
and Ramón García-Marín 

Department of Geography, Campus La Merced, University of Murcia, 30001 Murcia, Spain;  
adaniel.ibarra@um.es (D.I.-M.); franbel@um.es (F.B.-S.); ramongm@um.es (R.G.-M.)

\* Correspondence: gabp1@um.es



**Citation:** Ibarra-Marinas, D.; Belmonte-Serrato, F.; Ballesteros-Pelegrín, G.A.; García-Marín, R. Evolution of the Beaches in the Regional Park of Salinas and Arenales of San Pedro del Pinatar (Southeast of Spain) (1899–2019). *ISPRS Int. J. Geo-Inf.* **2021**, *10*, 200. <https://doi.org/10.3390/ijgi10040200>

Academic Editors: Wolfgang Kainz, Cristina Ponte Lira and Rita González-Villanueva

Received: 12 February 2021

Accepted: 23 March 2021

Published: 25 March 2021

**Publisher's Note:** MDPI stays neutral with regard to jurisdictional claims in published maps and institutional affiliations.



**Copyright:** © 2021 by the authors. Licensee MDPI, Basel, Switzerland. This article is an open access article distributed under the terms and conditions of the Creative Commons Attribution (CC BY) license (<https://creativecommons.org/licenses/by/4.0/>).

**Abstract:** Coastal erosion is an issue which affects beaches all over the world and that signifies enormous economic and environmental losses. Classed as a slow phenomenon, the evolution of the coastline requires long-term analysis. In this study, old cartography and aerial photographs from various dates have been used to study the evolution of the coastline. The information has been processed with free software (QGIS) and for the calculation of sediment transport the Coastal Modeling System (SMC) software. The results show the accretion/erosion phenomena that occurred after the construction of the port in San Pedro del Pinatar in 1954 and which changed the coastal dynamics of a highly protected area. In some sectors, the beach has been reduced almost in its entirety, with retreat rates of up to  $-2.05$  m per year and a total area loss of  $66,419.81$  m<sup>2</sup> in Las Salinas beach and  $76,891.13$  m<sup>2</sup> on Barraca Quemada beach.

**Keywords:** beach; coastal erosion; coastal construction; sediment transport; *Posidonia oceanica*

## 1. Introduction

The coastline is a highly dynamic area with constant movement of sediments that alter the morphological features of the coast and in which continuous changes take place in various spatial and temporal areas [1–3]. One of the most sensitive alterations is that caused by coastal erosion, which constitutes one of the greatest threats to coastlines worldwide [4] and which is currently being aggravated by mean sea level rise caused by climate change [5–7].

The process of coastal erosion consists of the permanent loss of sand from a littoral system and its magnitude depends on, to a great extent, the type of coastline, taking into account characteristics such as exposure to waves and their levels, or the composition and size of the sediments and the slope of the beach [8].

The causes of coastal erosion have their origin both in natural processes and in anthropogenic activities that influence coastal dynamics [9], especially if they intervene over a long period of time. It is also common for changes in the coastline to result from a combination of factors [10], such as rising sea levels, winds and storms, extraction of submerged sands for beach regeneration, and hydrological regulation of hydrographic basins. The latter is especially due to the construction of reservoirs, which retain sediments and limit their transport due to fluvial dynamics, the main beaches nourishment. Likewise, changes in land use in small coastal watersheds (coastal watercourses in the case of the Mediterranean) and their occupation limit the sedimentary transport and lead to the erosion of beaches fed by these variable hydrological systems [11–13]. Furthermore, coastal construction, such as promenades, but especially coastal structures that interfere with coastal transport, such as dikes and outer ports, constitute one of the most common causes and have the greatest impact on beach erosion [14]. In fact, the enormous effect

that coastal construction has on the coast [15] requires a more integrated and sustainable planning of ports and structural defenses through instruments such as Integrated Coastal Zone Management (ICZM). This tool allows optimizing both conservation and the use of resources, trying to satisfy the interests of all the agents involved, within a precise legal framework [16], and through an effective public policy [17].

Beyond regulative solutions, one of the options in response to coastal erosion is fixation through structures [8]. However, the artificialization of the coast reduces the natural capacity of the system to cope with phenomena such as a rise in sea level or storms [18]. In this sense, marshes and salt flats play a fundamental role in defending against floods, since they dissipate the energy of the tides and waves, reducing the height of the waves. Salt pans constitute a type of soft protection against engineering works, made of concrete or pebbles, considered hard protection and which, in the long term, are less sustainable. An abundant supply of sediment on beaches is essential for the survival of salt flats and against rising sea levels [19]. The loss of vegetation can also contribute to erosion, by destabilizing the sediment and increasing the exposure of salt flats, increasing damage during storms. On the other hand, the presence of breakwaters prevents this natural transgression, which causes habitats to be compressed between fixed defenses, a process known as coastal squeeze [20]. In this sense, beaches and dune systems acquire great value to avoid the loss of ecosystems that occur in salt flats and marshes.

One of the great natural allies against coastal erosion in the Mediterranean is the presence of *Posidonia oceanica*, aphanerogram seagrass that forms nearshore meadows, between 2 m deep and up to 40 m, since from that depth it is difficult to receive sunlight. The presence of this phanerogram seagrass serves to mitigate the effect of the waves on the sandy beaches [21], since part of the leaves that the plant loses in autumn accumulate on the beach, until they form a vegetal berm that increases the stability of the beach sediments [22], reducing wave energy. In addition, *Posidonia* meadows retain sand from submerged banks, which prevents the loss of sediment offshore [23].

The beaches of the Regional Park of the Salinas and Arenales of San Pedro del Pinatar, in the Region of Murcia, have seen their initial appearance altered, due to the interruption of the littoral transport of sediments, due to the construction in 1954 of the marina of San Pedro del Pinatar [24], from a small loading dock for the transport of salt built at the end of the 19th century.

The objective of this study was to analyze the evolution of the beaches of the Salinas and Arenales Regional Park of San Pedro del Pinatar between 1899 and 2019, evaluating the impact of the port on the dynamics of coastal transport and its effects on coastal erosion.

### Study Area

The coastal area studied runs from north to south between 37.79° and 37.84° north latitude and 0.75° east longitude (Figure 1). It has a total coastal length of 6.455 km (2.680 km are north of the port, where the beaches of El Mojón and Torre Derribada are located, and 3.275 km are south of the port, where the beaches of Las Salinas, Barraca Quemada and Punta de Algas are located). In addition, the port that separates both sections occupies 500 linear meters of coastline. The complex is part of the Regional Park of Salinas and Arenales of San Pedro del Pinatar, on the northern coast of the Region of Murcia (southeast of the Iberian Peninsula), which also includes all of the salt extractions area. The park can be considered to be made up of “hanging beaches” [25,26], formed by the accumulation of unconsolidated sediments on a rocky outcrop. These layers represent a limitation to the height of the waves that reach the shore of the beach. Considering their morphodynamic state [27], all the beaches in the park are dissipative.



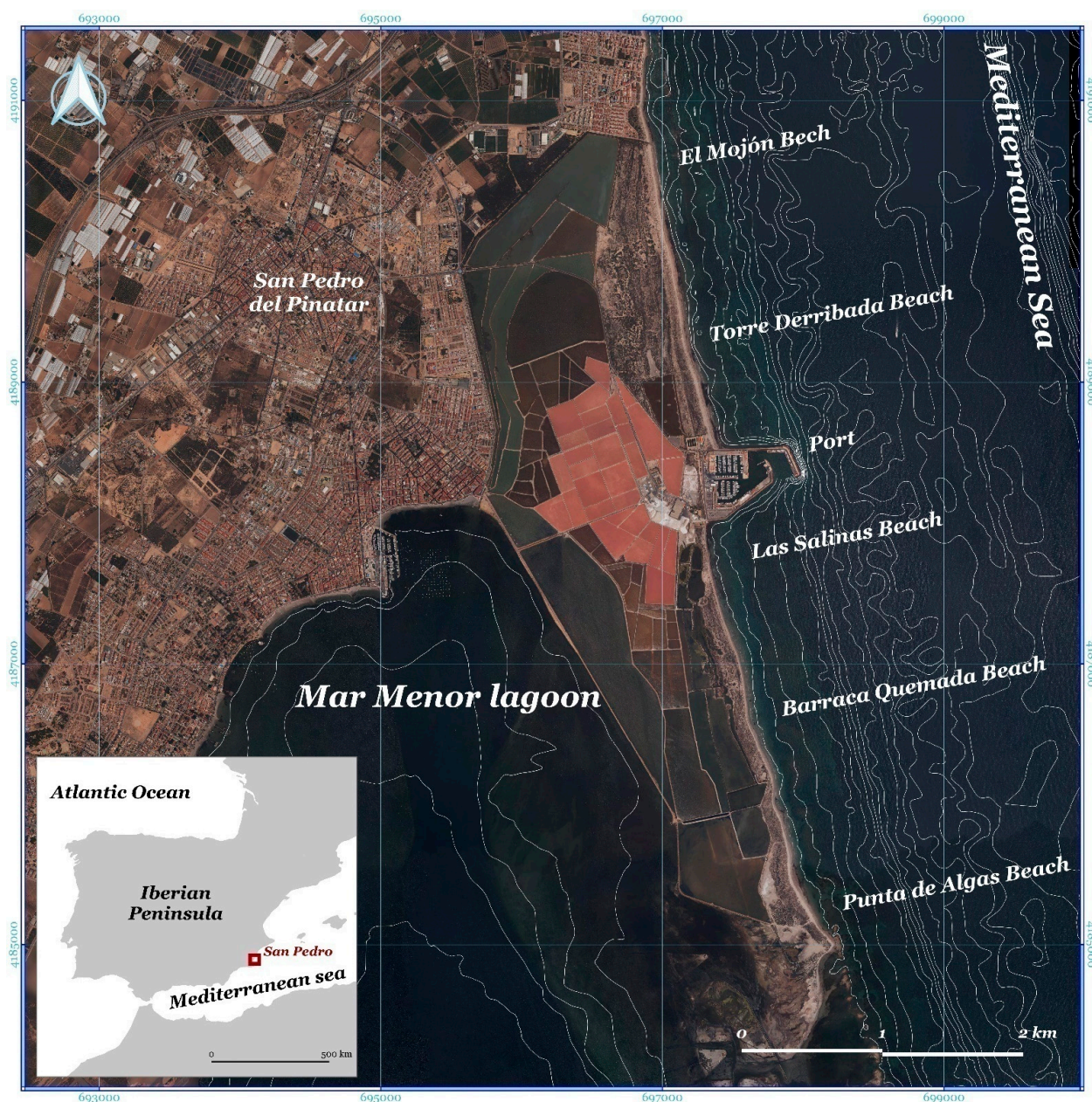


**Figure 1.** Regional Park of Salinas and Arenales of San Pedro Del Pinatar Beaches. Source: own elaboration.

The regional park covers an area of 856 hectares and belongs to the Natura 2000 Network and is classified as a Specially Protected Area of Mediterranean Importance (ZEPIM). Therefore, it is an area of great environmental relevance largely to the salt industry, since the salt flats have prevented the urbanization of this sector of the coast, despite the pressure for construction of the Spanish Mediterranean coast.

The beaches mainly receive waves from the NE–E sector, with the probability of occurrence of 13.72% for the NE cases, 17.39% for the ENE waves, and 15.64% for those of the E. In addition, the SSW waves also have an important probability of occurrence (11.88%).

The waves are not very energetic and the significant wave height is 0.8 m; in fact, the low energy of the waves is one of the keys that allows it to maintain a dissipative profile [28]. The coastline is oriented perpendicular to the ENE, in such a way that the waves coming from the ENE do not undergo hardly any refraction and are those that undergo the least energy reduction before the break. The submerged beach is characterized

by the presence of *Posidonia oceanica*, and the meadows are notably wide due to the low slope of the bathymetry in this area of the coastline.

## 2. Materials and Methods

### 2.1. Software Used

Two software tools have been used for the treatment of images and generation of cartography as well as the digitization of the coastline and generation of transects. On the one hand, for the calculation of sediment transport, Coastal Modeling System (SMC) software has been used. This software was developed by the Institute of Environmental Hydraulics of the University of Cantabria [29], which contains a wide set of numerical models, database methodologies, and which allows issues related to the coasts to be addressed.

The QGIS Geographical Information System [30] has been used to process spatial information.

### 2.2. Sediment Transport Models and Active Depths

The models used for this purpose were the Coastal Engineering Research Center (CERC) model and a variation of it [31]. The CERC model is based on the assumption that the total sediment transport rate along the coast is proportional to the flow of energy along the coast:

$$Sc = A * H_{s0}^2 * c_0 * K_r^2 * \sin\theta_b * \cos\theta_b \quad (1)$$

where:  $Sc$  is the transport of sand in  $m^3/s$ ;  $A$  is a coefficient dependent on the type of beach;  $c_0$ , the speed of the wave in deep water in  $m/s$ ;  $\theta_b$ , the angle between the depth contours and the crest of the wave in the surf zone;  $H_{s0}$ , the significant wave height in deep water in  $m$ ; and  $K_r$  is the coefficient of refraction.

The Kamphuis model is a variant of the CERC formula that includes the effects of the wave period, known as wave slenderness [31,32], the slope of the beach, and the diameter of the grain. In the Kamphuis model, the longitudinal sediment transport rate can be expressed as:

$$Q_s = \int (H, T, h, \rho, \mu, g, x, y, z, \rho_s, D) \quad (2)$$

where:  $Q_s$  is the sediment transport rate, expressed in  $kg/s$ ;  $H$ , the wave height;  $T$ , the period of the wave;  $h$ , the depth;  $\rho$ , the density of water;  $\mu$ , the dynamic viscosity of water;  $g$  acceleration due to gravity;  $x, y, z$  are directions;  $t$  is time;  $\rho_s$ , the density of the sediment; and  $D$  the diameter of the sediment, which has been calculated using the sieve from the samples obtained from the beaches of the study area.

In order to analyze the impact of the Port of San Pedro del Pinatar on sediment transport, the coastal depth of the beach profile ( $d_l$ ) has been calculated from the wave height, which exceeds 12 h per year [33]. Its calculation is obtained from the expression:

$$d_l = 1.75 * H_{12} - 57.90 * \frac{H_{12}^2}{G * T_z^2} \quad (3)$$

where:  $d_l$  is the littoral depth in  $m$ ;  $H_{12}$  is the significant wave height in  $m$ ;  $G$ , the acceleration of gravity in  $m/s^2$ ;  $T_z$  means the average period.

From the littoral depth, which indicates the longitudinal transport of sediments, the depth of shoal has been defined, which determines the limit of transverse transport of sediments [34]:

$$d_s = 2 * d_l \quad (4)$$

where:  $d_s$  is the depth of shoaling and  $d_l$  the coastal depth of the beach profile. Once the active depths have been obtained, the sediment transport zones have been mapped from bathymetry lines of 1 m resolution, corresponding to the year 2013. Although the bathymetry is temporally highly variable.



### 2.3. Cartography and Aerial Photographs

Despite their limitations, archival topographic maps can be useful in the investigation of changes in the coastline [35]. There are potential errors associated with this mapping, including variations in scale, datum changes, projection failures, or different topographic standards. However, many of them can be resolved through different treatments and, on many occasions, as is the case of the beaches of the Regional Park of Las Salinas and Arenales of San Pedro del Pinatar, they constitute the only source of data available for certain dates.

To carry out the following study, the cartography of San Pedro del Pinatar has been georeferenced from the topographic studies carried out in August 1899 by the Geographical and Statistical Institute at a scale of 1:25,000.

Due to the microtidal character of this area and the fact that the aerial photographs used were taken in summer, the error due to seasonal sea level fluctuations can be considered insignificant.

Aerial photographs corresponding to the years 1956, 1981, and 2017 have been used for digitization. The coordinate reference system used was ETRS89 UTM30N.

### 2.4. Definition and Digitization of the Beach Surface and Coastline

Two proxies have been used with different criteria and with two objectives: the first was the calculation of the distances between the coastline distances at different dates, understood as the erosion or setback of each sector. The second was the calculation of the variations of the beach area.

To analyze the variability of the coastline, a definition is required, taking into account the techniques and available data [36]. For this study, the shoreline definition is the line that marks the boundary between the sea and the land, regardless of the criteria chosen for its representation and refers to the Mean High Water (MHW) shoreline.

### 2.5. Generation of Transects

QGIS Station Lines' plugin [37] has been used for transects generation. This plugin allows the creation of lines along polylines, from certain parameters (length, side, angle), and assuming a Cartesian coordinate system. In this study, transects have been generated every 15 m.

### 2.6. Areas, Distances, and Erosion Rates

As a preliminary step to calculating the rates, distances have been calculated with the Shoreline Change Envelope (SCE) and Net Shoreline Movement (NSM). The first is the existing longitude between the most distant coastlines for each transect, that is, without taking into account the dates. The NSM shows the distance between the oldest and newest coastlines, and since it does not use any other information between dates, the results of the NSM calculation are considered an end point measure.

The calculation of rates is one of the most used monitoring indicators in the transition zone between the marine and terrestrial environment. To calculate the rates of variation of the coastline from previously digitized data, it is common to apply various statistical methods, such as the end point rate, the average of the rates, the linear regression rate, or the rate of jackknife [38–40]. In this study, the annual rate of change, End Point Rate (EPR), has been used, which represents the rate of change that the coast has suffered, expressed in meters per year. For its calculation, the net distance is used, divided by the number of years that separate the dates of the coastlines obtained in the digitization.

### 2.7. Calculation of Errors in Digitization from Aerial Photographs

Due to the micro-tidal nature of the study area [41,42], tidal fluctuation has not been incorporated into this study. Nevertheless, it has been considered necessary to calculate three error components [42] for the digitized coast from aerial photographs:

- i. Digitization error: error associated with the coastline digitization process. The digitization has been repeated several times by a single specialist. The error has been calculated from the standard deviation of them.
- ii. Error in geometric correction: expressed as the mean square error of the rectification process [43]. It is the distance between the control points established in the aerial photographs.
- iii. Scanning or pixel error: represented by the resolution of the different images [44]. The larger the pixels, the greater the uncertainty in the interpretation of the coastlines. For this purpose, the length of the pixel side is used.

Finally, once the three errors have been calculated, they have been computed as the square root of the squared sum of each component [15].

### 3. Results

#### 3.1. Drift, Sediments, and Depth

From the Coastal Modeling System (SMC) software, it has been possible to calculate the net transport of sediments from the littoral system. Without artificial obstacles, the sand would be distributed from north to south with volumes of  $1,096,030 \text{ m}^3/\text{year}$  according to the CERC model, and  $238,270 \text{ m}^3/\text{year}$  based on the Kamphuis model. There are seasonal differences: in the month of July transport is practically nil, however, transport in the opposite direction to general littoral drift is practically nil all year round. The calculation of the active depths has made it possible to analyze the shadow effect of the port facilities. In the case of the beaches in the study area, the coastal depth, in which huge changes in the profile occur due to both longitudinal and transverse transport, is located at 5.60 m, according to the Hallermeier model, which determines that the closure depth is 11.20 m. The Port of San Pedro exceeds the active depth (Figure 2), which represents a barrier with the capacity to interrupt the longitudinal transport of sediments.

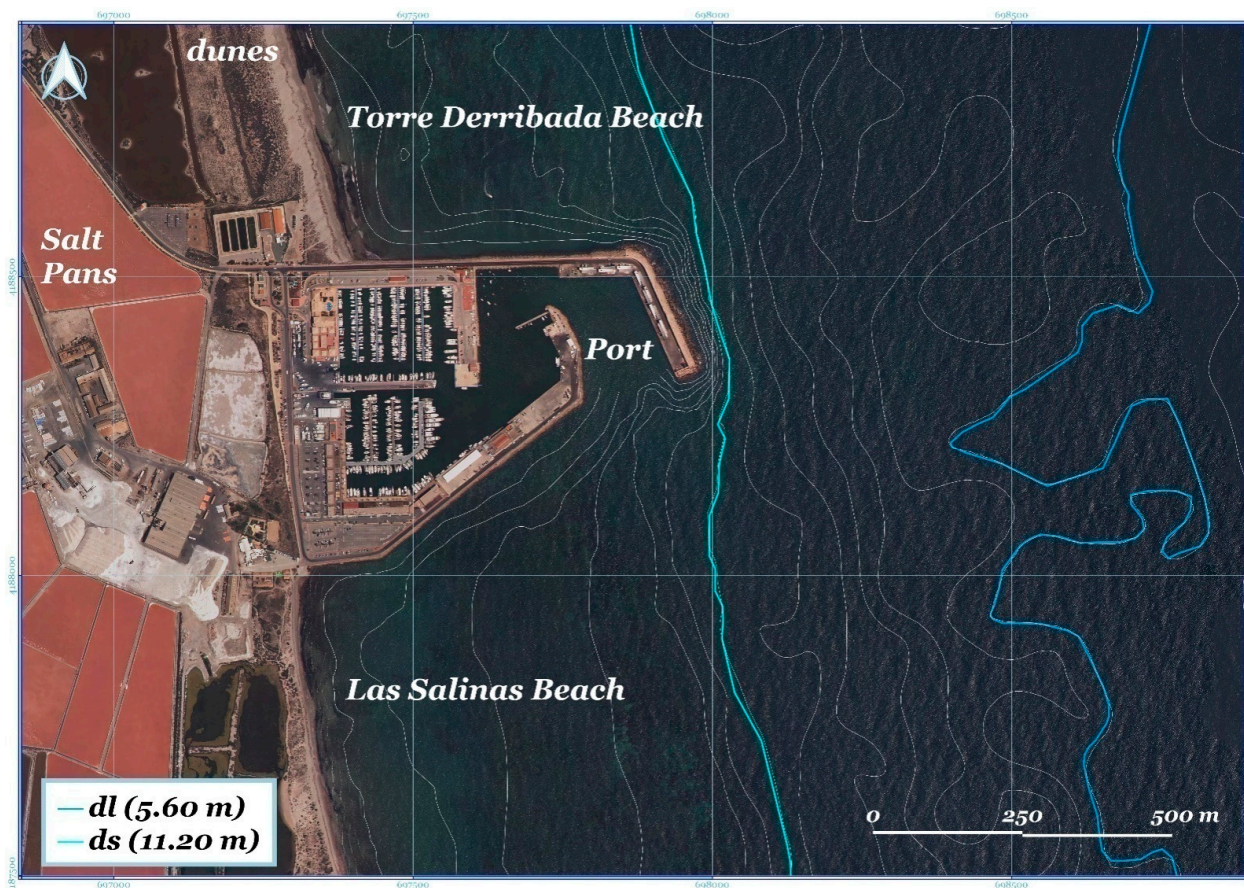


Figure 2. Coastal depth and shoal in the surroundings of the Port of San Pedro del Pinatar. Source: own elaboration.

This interruption of the longitudinal transport of N–S sediments has had very negative consequences on the southern beaches, in addition to the degradation of the dune system; especially the one associated with the beaches of Las Salinas and Barraca Quemada, located immediately to the south of the port, in addition to being the beaches that register the greatest loss of sand. This intensity of use is transferred to the dune system, which has been affected by a dense network of trails that have caused intense erosion. In addition to both circumstances, there is also the rise in sea level as a consequence of climate change. In this sense, and taking into account the evolution of draughts in the Mediterranean area, the beaches and dunes of the Salinas Regional Park and San Pedro del Pinatar are in danger of disappearing in the coming decades.

### 3.2. Erosion and Accretion of the Beaches of the Salinas and Arenales Regional Park in San Pedro del Pinatar

From the digitization of the beaches' areas per year, the surface variations of the beaches in the study area and the inter-annual variations associated with each period (Table 1) have been obtained.

**Table 1.** Inter-annual variations of the surface by beach and period.

Beach	Sector	1899–1956 (m <sup>2</sup> /Year)	1956–1981 (m <sup>2</sup> /Year)	1981–2016 (m <sup>2</sup> /Year)	1899–2016 (m <sup>2</sup> /Year)
El Mojón	1	−56.06	7.24	−200.64	−63.65
Torre Derribada	2	768.66	1954.33	2227.66	1191.52
Salinas	3	1926.54	−4596.64	−1913.24	−553.50
Barraca Quemada	4	−765.59	−663.11	−881.36	−640.76
Punta de Algas	5	−131.35	−396.47	635.97	−4.83
TOTAL		1742.21	−3694.65	−131.60	−71.22

The greatest surface losses are related to the shadow effect of the port, the beaches of Las Salinas and Barraca Quemada have surface losses in all periods, but these soar after the construction of the dikes. Torre Derribada beach, despite lacking sediment feeding, increases its width due to the accumulation of sand in the Levante dike located south of the beach.

### 3.3. Sections Located North of the Port

On the beaches located to the north of the port, El Mojón and Torre Derribada beach (Figure 3), the N–S littoral drift, and the obstacle that the port poses to the longitudinal transport of sediments, affects both beaches differently.

The 45 observations of El Mojón beach (Figure 4a), located at the northern end of the park, show slow erosion ( $EPR = -0.10$  m/year). The average rates are in equilibrium in the periods 1899–1956 with an inter-annual rate of  $-0.09$  m/year and 1956–1981 ( $-0.04$  m/year), however, it has increased in the last period 1981–2016 ( $0.20$  m/year). In this period, the average width of the beach undergoes an important negative evolution, since it goes from 32.66 m to 25.85 m.

The total loss of sediment is related to the lack of supply within the system. The perimeter channel of Las Salinas, which connects the lagoon of the Mar Menor with the Mediterranean, has no supply capacity and the mouths of watercourses and rivers that were related to the original formation of the beaches have lost their connection with the littoral system, due to the increased sealing of the soil of the small sub-basins of the coastal watercourses and, above all, to the construction of the ports located in the south of the Province of Alicante and to the extreme regulation of the River Segura, whose mouth is 30 km north of the regional park.



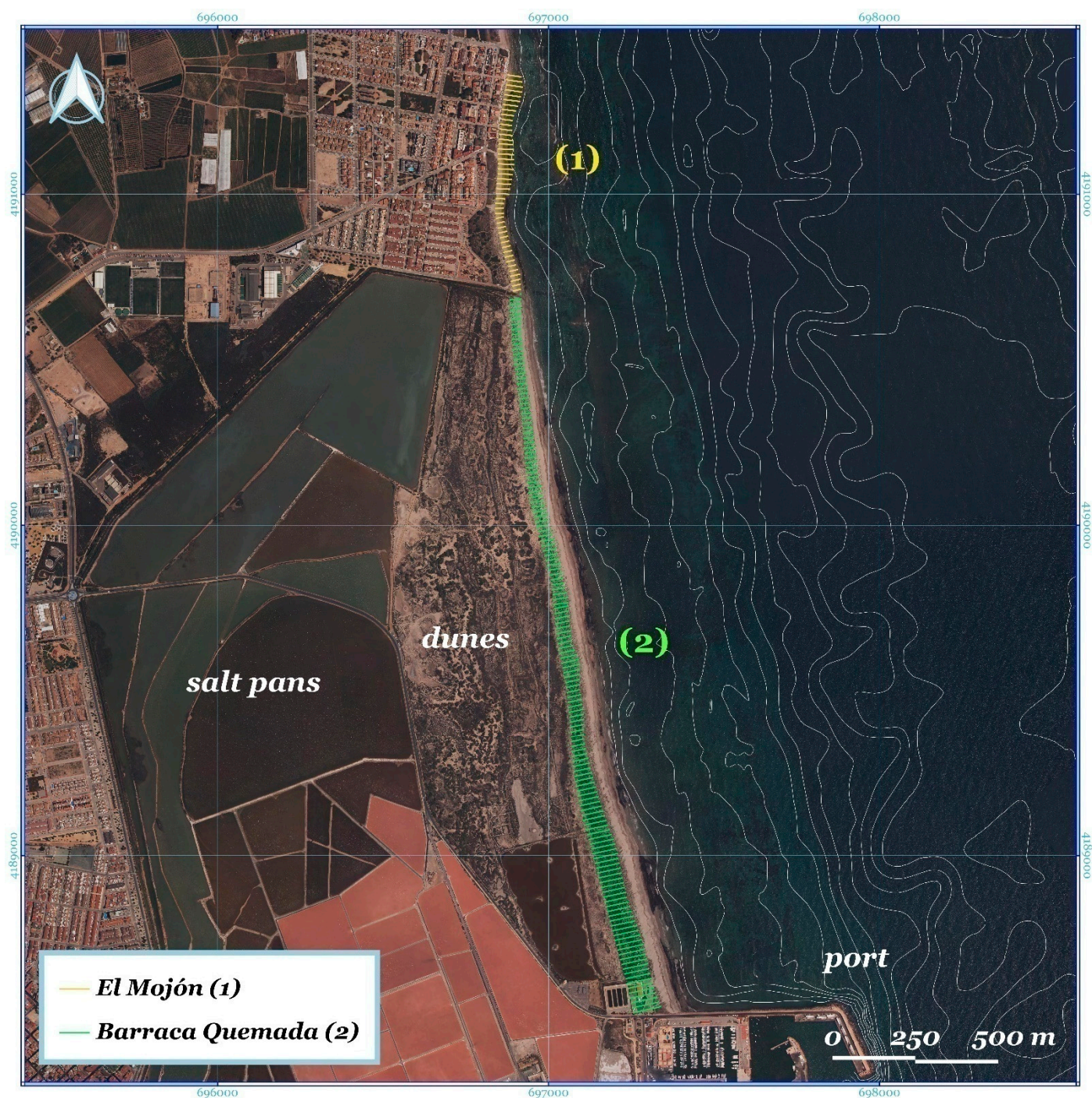


**Figure 3.** Sections located north of the Port of San Pedro del Pinatar. El Mojón Beach (1) and Torre Derribada Beach (2). Source: own elaboration.

At Playa de la Torre Deribada (Figure 4b), the average width of the beach has increased by 64.40 m on average. The rates, which have been obtained from 149 proxies, are positive in the period 1899–1956 (0.30 m/year), but from the construction of the Port of San Pedro del Pinatar they skyrocket. In the period 1956–1981, growth was the highest (0.89 m/year) and, despite the slowdown in the accretion phenomenon in recent decades, the rate for the period 1981–2016 reached 0.72 m/year. In 120 years, Torre Deribada beach has increased its width by 0.55 m per year. The beach does not receive depositions, but it does remain embedded in the port, which has influenced in recent years the difference between the northern part with a slight erosive trend and the southern part with an accretion of more



than 1 m/year in its last 800 m, where sediment transport accumulates following the direction of the drift.

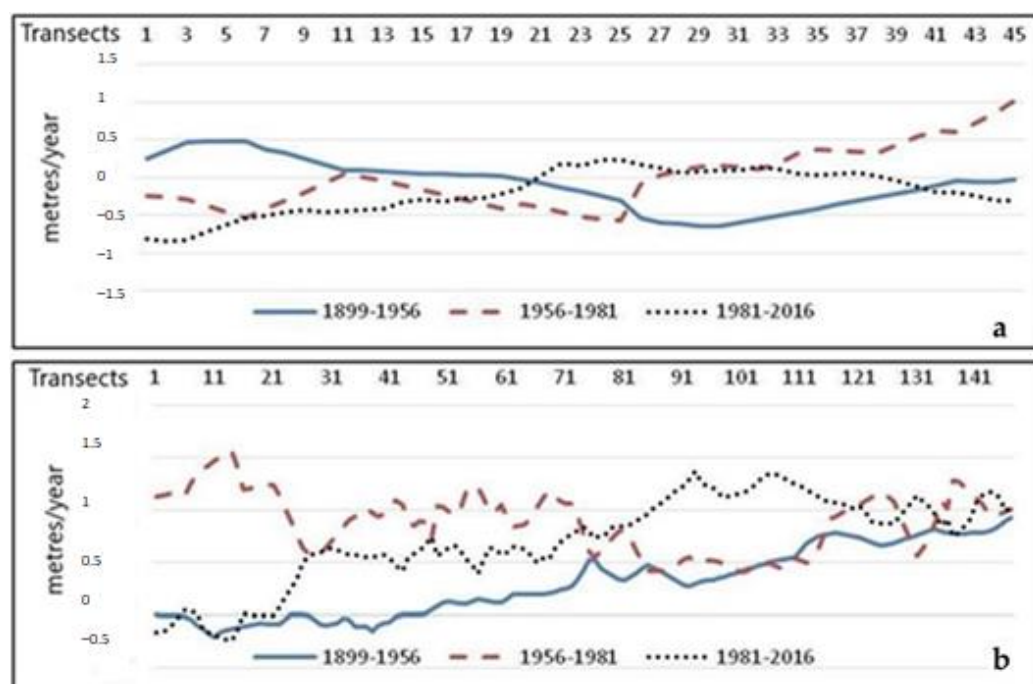


**Figure 4.** Shoreline variation rates evaluated along the transects in the beaches of El Mojón (a) and Torre Derribada (b).

### 3.4. Sections Located South of the Port

The erosive processes on the beaches of Las Salinas, Barraca Quemada and Punta de Algas (Figure 5) slow down in the middle of the first decade of the 21st century, especially with the cessation of the removal of berms of *Posidonia oceanica* in 2006 and the contribution of 14,500 m<sup>3</sup> of sand from 2010 carried out by the Ministry of Agriculture, Fisheries, Food and Environment.

Las Salinas beach expands towards the south from the western dock of Puerto de San Pedro, which is why, since the enlargement of the facilities, it has suffered intense erosion. For the analysis of this beach, there were 80 proxies (Figure 6a), which show, firstly, how the beach increased its width by 14.40 m in the first period (1899–1956). The western dike generates a transport of the waves towards the south and consequently a local retreat of the coastline. Furthermore, the eastern swell is reflected by changing the propagation of the wave fronts and the energy flow, causing the coastline to have undergone a rotation since the construction of the port.

The following period (1956–1981) began two years after the expansion of the port, which, until then, only had a pier. Over 25 years, the width lost 30.56 m on average, which became 40.22 m between 1981 and 2016. The rates of the last periods (−1.22 m/year and −1.15 m/year) exceed the meter of annual loss, the maximum is in the first period: −2.05 m/year. Las Salinas beach, the most visited due to its accesses, has grown from an average width of 77.74 m at the end of the 19th century to 21.37 m today (2016).

The analysis of the Barraca Quemada beach has been carried out from 98 transects between the beaches of Las Salinas and Punta de Algas (Figure 6b). The mean length of the Barraca Quemada beach was 78.06 m in 1899, with a maximum of 117.70 m. Throughout the 20th century, accretion/erosion rates have always been negative and almost constant: 0.45 m/year between 1899 and 1956, 0.43 m/year between 1956 and 1981, and 0.42 from 1981 to the present, despite regeneration. Today (2016), the average width of the beach is 26.56 m.

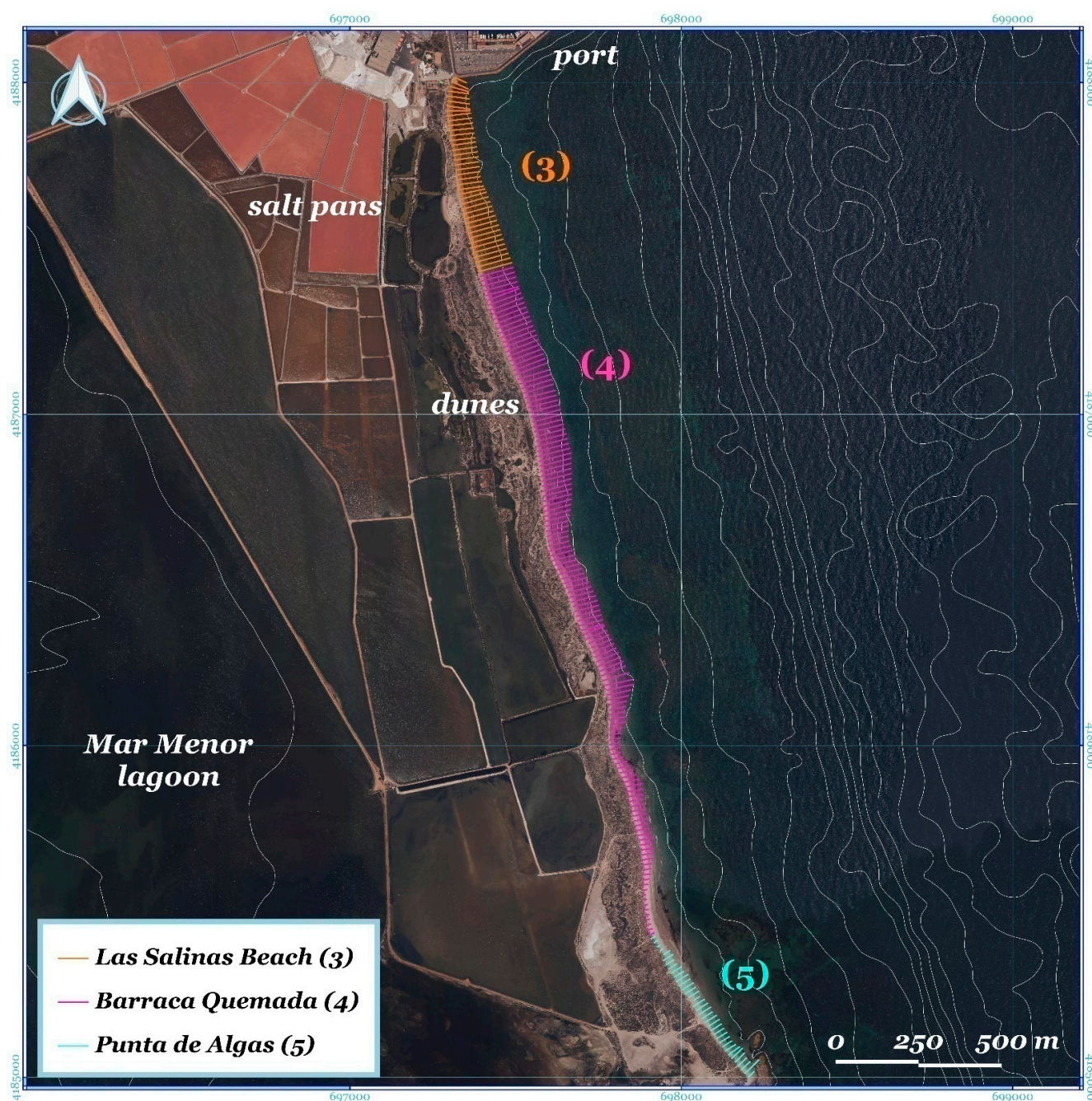


**Figure 5.** Sections located south of the Port of San Pedro del Pinatar. Las Salinas Beach (3), Barraca Quemada Beach (4), and Punta de Algas Beach (5). Source: own elaboration.

The 33 southernmost transects correspond to Punta de Algas beach (Figure 6c). In this sector, the width of the beach has increased since the 1980s, due to the accumulation of sand carried by the coastal drift towards the south, where they have run aground in the rocky outcrops, although much of the sediment leaves the system and is deposited in Las Encañizadas, a channel that connects the Mediterranean Sea with the Mar Menor, whose width has decreased due to clogging. The width of the beach decreased by 13.80 m in the first 50 years. In the period between 1956 and 1981, regression increased by 42.53 m, which corresponds to a rate of  $-1.70$  m/year. The rate has become positive in recent decades ( $1.44$  m/year), creating a situation of apparent equilibrium ( $EPR = -0.05$  m/year) for the 120 years studied.



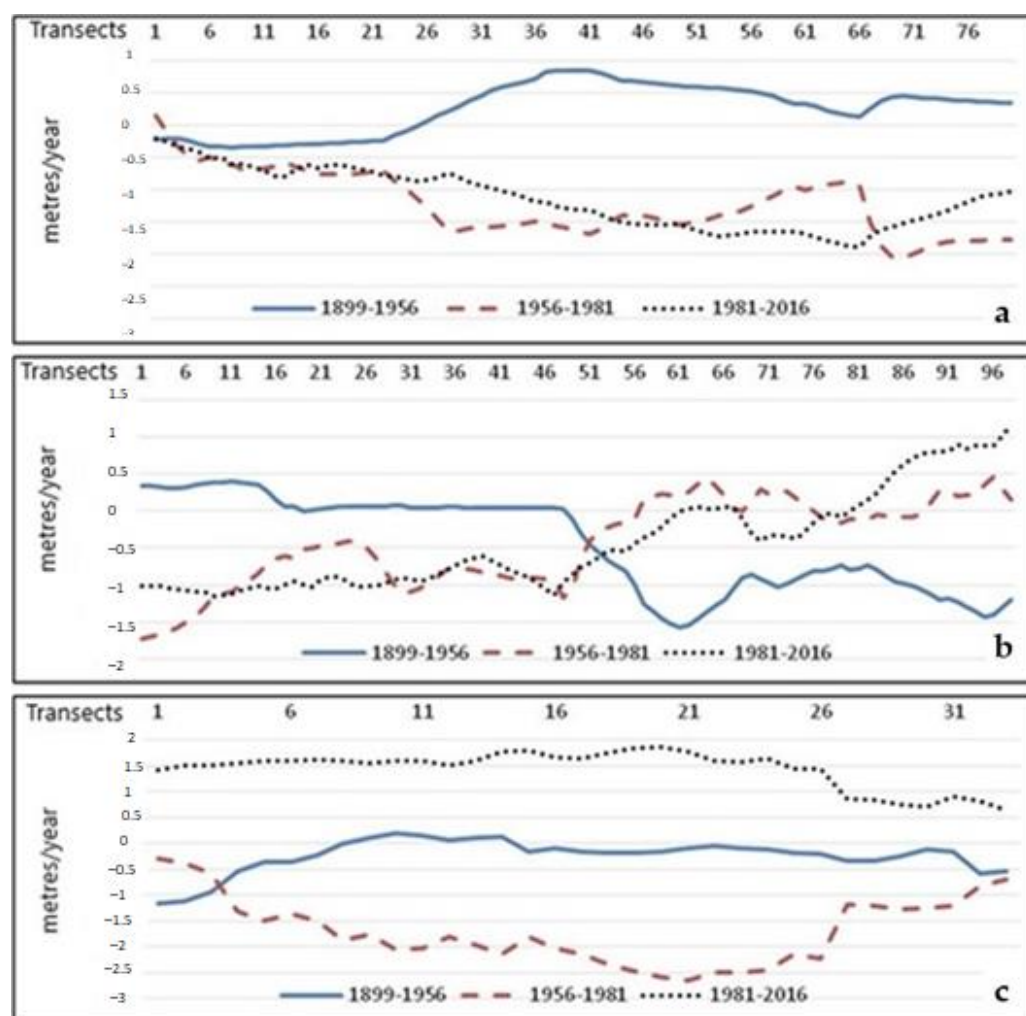


**Figure 6.** Shoreline variation rates evaluated along the transects in the beaches of Las Salinas (a), Barraca Quemada (b), and Punta de Algas (c). Source: own elaboration.

#### 4. Discussion

In general terms, the Spanish Mediterranean coastline is in an erosive state, the main causes being of anthropic origin [45–47]. In the southeast of the Iberian Peninsula, the lack of feeding from the watercourses is the main cause of coastal erosion [12,48]. Changes in land use and in the hydrography of the littoral basins mean modifications important enough to change the direction of the sediments that feed the beaches.

The interruption of sediment transport caused by port facilities, in most cases gained from the sea [49], is usually one of the most common origins of beach erosion on the Mediterranean coast. Coastal construction, especially that of ports, due to their size, is one of the main causes of alteration of the coastal dynamics in the transport of sediments, as happens, for example, in the beach of Sa Ràpita, located on the south coast of Mallorca. The beaches in this area have suffered the shadow effect of the port built in 1977 [42].

In the case of the beaches of San Pedro del Pinatar, both the decrease in the contribution of sediments (for the reasons mentioned above) and the construction of the port have unbalanced the natural dynamics of the system, with great differences between the beaches located at Barlomar and Sotamar port.

The importance of maintaining some salt flats in this area is essential to try to control coastal erosion. One of the main objectives of the salt exploitation restoration plans is related to the creation of sustainable sites that facilitate continuous ecological and natural succession, a development that has been shown to be successful elsewhere since the 1990s [50]. In addition to the fundamental role as a support for marine fauna and its

capacity to capture CO<sub>2</sub> [51], one of the most forceful responses to coastal erosion is the adequate conservation of oceanic posidonia [22,52], due to its active role in coastal dynamics. The removal of dead leaves tends to become a common problem [49], since it means the disappearance of a defense against storms, which usually appear when the leaves fall and accumulate on the shore.

Updrift port of San Pedro del Pinatar, the LIFE-Salinas Project, funded by the European Union is being developed between 2018 and 2022 (LIFE17/ES/000184). It has carried out stabilization and reinforcement of more than 2 hectares of dune system along the first 600 m of beach, which includes a preferential restoration of priority conservation habitats in the European Union (1510 “Saline Steppes” and 2250 “Littoral dunes with *Juniperus* spp.”). For this, a network of sand fences and sand collectors made of cane (*Arundodonax*), with an approximate length of 3000 m, arranged in an orientation perpendicular to the prevailing wind direction, have been installed, together with the elimination of the network of existing trails and the closure of access to people in the most vulnerable dunes [53].

Using open-source software has several benefits. Beyond being free software, free source Geographical Information Technologies have great versatility, which allows the modification of the software itself to adapt it to the specific needs of each project or study [54]. In addition, this type of software is continually improving due to contributions from the scientific community. The transects between coastlines from different dates with GIS software is a widely used method in studies of coastal erosion. Among the most outstanding tools available, the Digital Shoreline Analysis DSAS is worth mentioning. It is software developed by the U.S. Geological Survey which is often used in coastal evolution studies. However, this software is not compatible with QGIS, so, as an alternative, the QGIS Station Lines plugin has been used.

The use of aerial photographs is widely extended in coastal dynamics and coastal erosion studies [55–59]. Aerial photographs are compared and it is necessary to know if the profile corresponds to periods of fair weather or storms on each date. On sandy beaches, during fair conditions, low waves provide sediment that accumulates on the beach [60], while during high-energy and storm conditions there is a loss of sediment through the rip currents, which are generated in the area of breakers and compensate for the effect of over-elevation caused by the waves [61]. One of the advantages of using aerial photography on micro-tidal beaches is that the problem of defining the coastline is avoided.

## 5. Conclusions

The use of Geographic Information Technologies is essential in research studies for the analysis of coastal erosion, since it allows evaluation of the effects of coastal dynamics, especially through the study of the historical evolution of the position of the coastline.

The construction of the port of San Pedro del Pinatar represents a fundamental change in the natural sedimentary dynamics of the adjacent beaches, with accretion in the northern sector, which contrasts with significant erosion processes in the beaches located to the south.

Due to the lack of depositions and the shadow effect of the port, the current erosive state of the downdrift beaches of the regional park is serious enough that there is a need to adopt adequate management measures to prevent the disappearance of the beaches and the system of dunes.

In this sense, free software from Geographic Information Systems is deemed reliable and may successfully address any type of geographical study thanks to the open-source libraries developed by the scientific and professional community.

**Author Contributions:** Conceptualization, Daniel Ibarra-Marin, Francisco Belmonte-Serrato, Gustavo A. Ballesteros-Pelegrín and Ramón García-Marín; methodology, Daniel Ibarra-Marin and Francisco Belmonte-Serrato; formal analysis, Daniel Ibarra-Marin, Gustavo A. Ballesteros-Pelegrín, and Ramón García-Marín; investigation, Daniel Ibarra-Marin, Francisco Belmonte-Serrato, Gustavo A. Ballesteros-Pelegrín and Ramón García-Marín; data curation, Daniel Ibarra-Marin and Ramón García-Marín; writing—original draft preparation, Francisco Belmonte-Serrato, Daniel Ibarra-Marin, Gustavo A. Ballesteros-Pelegrín and Ramón García-Marín; writing—review and



editing, Daniel Ibarra-Marinas, Francisco Belmonte-Serrato, Gustavo A. Ballesteros-Pelegrín and Ramón García-Marín; supervision, Ramón García-Marín. All authors have read and agreed to the published version of the manuscript.

**Funding:** This research was funded by the Environment and Climate Action Program (LIFE), managed by the European Commission, grant number LIFE17 NAT/ES/000184, and the APC was funded by the same project. The LIFE-SALINAS Project, Conservation of habitats and aquatic birds in the LIC (Community Interest Area) and ZEPA (Special Areas for the Protection for Birds) ES0000175 “Salinas y Arenales de San Pedro del Pinatar” (Southeastern Spain), is based on sustainable development, since it improves the conservation of priority fauna species and habitats in the European Union, in addition to enhancing the ecosystem services by increasing production and improving the quality of salt. More information about the Project at: <https://lifesalinas.es/> (accessed on 24 March 2021).

**Institutional Review Board Statement:** Not applicable.

**Informed Consent Statement:** Not applicable.

**Data Availability Statement:** Not applicable.

**Acknowledgments:** This article has been written thanks to the co-financing of LIFE funds from the European Union, through the LIFE17 / ES / 000184 Project, Conservation of habitats and aquatic birds in the LIC and SPA ES0000175 “Salinas and Arenales of San Pedro del Pinatar” (LIFE-SALINAS). Authors want to thank the anonymous reviewers for their suggestions, which have helped to significantly improve the manuscript.

**Conflicts of Interest:** The authors declare no conflict of interest.

## References

1. Absalonsen, L.; Dean, R.G. Characteristics of the shoreline change along Florida sandy beaches with an example for Palm Beach County. *J. Coast. Res.* **2011**, *27*, 16–26. [\[CrossRef\]](#)
2. Del Río, L.; Gracia, F.J.; Benavente, J. Shoreline change patterns in sandy coasts. A case study in SW Spain. *Geomorphology* **2013**, *196*, 252–266. [\[CrossRef\]](#)
3. Jackson, D.W.T.; Short, A. *Sandy Beach Morphodynamics*; Elsevier: Amsterdam, The Netherlands, 2020.
4. Xue, Z.; Feng, A.; Yin, P.; Xia, D. Coastal erosion induced by human activities: A northwest Bohai Sea case study. *J. Coast. Res.* **2009**, *25*, 723–733. [\[CrossRef\]](#)
5. Zhang, K.; Douglas, B.C.; Leatherman, S.P. Global warming and coastal erosion. *Clim. Chang.* **2004**, *64*, 41. [\[CrossRef\]](#)
6. Dieng, H.B.; Cazenave, A.; Meyssignac, B.; Ablain, M. New estimate of the current rate of sea level rise from a sea level budget approach. *Geophys. Res. Lett.* **2017**, *44*, 3744–3751. [\[CrossRef\]](#)
7. Nerem, R.S.; Beckley, B.D.; Fasullo, J.T.; Hamlington, B.D.; Masters, D.; Mitchum, G.T. Climate-change—driven accelerated sea-level rise detected in the altimeter era. *Proc. Natl. Acad. Sci. USA* **2018**, *115*, 2022–2025. [\[CrossRef\]](#)
8. Van Rijn, L.C. Coastal erosion and control. *OceanCoast. Manag.* **2011**, *54*, 1–21. [\[CrossRef\]](#)
9. Masria, A.; Iskander, M.; Negm, A. Coastal protection measures, case study (Mediterranean zone, Egypt). *J. Coast. Conserv.* **2015**, *19*, 281–294. [\[CrossRef\]](#)
10. Doody, P.; Ferreira, M.; Lombardo, S.; Lucius, I.; Misdrop, R.; Neising, H.; Salman, A.; Smallegange, M. *Living with Coastal Erosion in Europe: Sediment and Space for Sustainability—Results from the Erosion Study*; EUCC: Leiden, The Netherlands, 2004.
11. López Bermúdez, F.; Gomariz Castillo, F. Las ramblas, agentes reguladores del litoral mediterráneo ibérico. El ejemplo de la rambla de las Moreras. Murcia. In *Geomorfología litoral i Quaternari*; Eulàlia, S., Joan, F.M., Eds.; Publications of the University of Valencia (PUV): Valencia, Spain, 2006; pp. 245–257.
12. Belmonte-Serrato, F.; Romero Díaz, A.; Rupérez Tirado, E.; Moreno Brotóns, J. El impacto de la agricultura intensiva en el uso turístico de las playas de Marina de Cope (Murcia). *Cuad. Tur.* **2011**, *27*, 23–38.
13. Belmonte-Serrato, F.; Romero Díaz, A.; Ruiz Sinoga, J.D. Retroceso de la línea de costa en playas del sur de la Región de Murcia. *Scr. Nova* **2013**, *XVII*, 443.
14. Murali, R.; Babu, M.; Mascarenhas, A.; Choudhary, R.; Sudheesh, K.; Vethamony, P. Coastal erosion triggered by a shipwreck along the coast of Goa, India. *Curr. Sci.* **2013**, *105*, 990–996.
15. Fletcher, C.; Rooney, J.; Barbee, M.; Lim, S.; Richmond, B.M. Mapping shoreline change using digital orthophotogrametry on Maui, Hawaii. *J. Coast. Res.* **2003**, *38*, 106–124.
16. Shipman, B.; Stojanovic, T. Facts, fictions, and failures of integrated coastal zone management in Europe. *Coast. Manag.* **2007**, *35*, 375–398. [\[CrossRef\]](#)
17. Barragán Muñoz, J.M.; Chica Ruiz, J.A.; Pérez Cayeiro, M.L. Iniciativa andaluza (España) para la gestión integrada de zonas costeras (GIZC). *Rev. Geogr. Norte Gd.* **2008**, *41*, 5–22. [\[CrossRef\]](#)
18. Guisado Pintado, E.; Malvárez García, G.C. El estado morfodinámico de las playas a través de modelización numérica de propagación y asomeramiento del oleaje: El frente litoral de Doñana. *GeoFocus* **2015**, *15*, 163–180.

19. Moller, I.; Spencer, T. Wave dissipation over macro-tidal saltmarshes: Effects of marsh edge typology and vegetation change. *J. Coast. Res.* **2002**, *36*, 506–521. [\[CrossRef\]](#)
20. Adam, P. Saltmarshes in a time of change. *Environ. Conserv.* **2002**, *29*, 39–61. [\[CrossRef\]](#)
21. Pethick, J. Coastal management and sea-level rise. *Catena* **2001**, *42*, 307–322. [\[CrossRef\]](#)
22. Elginöz, N.; Kabdaslit, M.S. Effects of Posidonia Oceanica Seagrass Meadows on Storm Waves. *J. Coast. Res.* **2011**, *64*, 373–377. [\[CrossRef\]](#)
23. Gómez-Pujol, L.; Orfila, A.; Álvarez-Ellacuría, A.; Terrados, J.; Tintor, J. Posidonia oceanica beach-cast litter in Mediterranean beaches: A coastal videomonitoring study. *J. Coast. Res.* **2013**, *65*, 1768–1773. [\[CrossRef\]](#)
24. Hemminga, M.A.; Nieuwenhuize, J. Seagrass Wrack-induced Dune formation on a tropical coast. *Estuarine. Coast. Shelf Sci.* **1990**, *31*, 499–502. [\[CrossRef\]](#)
25. Ballesteros-Pelegrín, G.A. *El Parque Regional de las Salinas y Arenales de San Pedro del Pinatar. Actividades Humanas y Conservación*; Universidad de Murcia: Murcia, Spain, 2014; Volume 512, p. 367.
26. Larson, M.; Kraus, N.C. Representation of non erodible (hard) bottoms in beach profile change modeling. *J. Coast. Res.* **2000**, *16*, 1–14.
27. Gallop, S.L.; Bosserelle, C.; Pattiaratchi, C.B.; Eliot, I. Hydrodynamic and morphological response of a perched beach during sea breeze activity. *J. Coast. Res.* **2011**, *64*, 75–79.
28. Wright, L.D.; Short, A.D. Morphodynamic Variability of Surf Zones and Beaches: A Synthesis. *Mar. Geol.* **1984**, *56*, 93–118. [\[CrossRef\]](#)
29. Wright, L.D.; Chappell, J.; Thom, B.G.; Bradshaw, M.P.; Cowell, P. Morphodynamics of reflective and dissipative beach and inshore systems: Southeastern Australia. *Mar. Geol.* **1979**, *32*, 105–140. [\[CrossRef\]](#)
30. Quetzalcóatl, O.; González, M.; Cánovas, V.; Medina, R.; Espejo, A.; Klein, A.; Tessler, M.A.; Almeida, L.R.; Jaramillo, C.; Garnier, R.; et al. SMC, a coastal modeling system for assessing beach processes and coastal interventions: Application to the Brazilian coast. *Environ. Model. Softw.* **2019**, *116*, 131–152. [\[CrossRef\]](#)
31. Qgis Development Team. QGIS Geographic Information System. Open Source Geospatial Foundation Project. 2019. Available online: <http://qgis.osgeo.org> (accessed on 25 November 2020).
32. Kamphuis, J.W. Alongshore Sediment Transport Rate. *Journal of Waterway, Port. Coast. Ocean Eng.* **1991**, *117*, 624–640. [\[CrossRef\]](#)
33. Córdova-López, L.F.; Torres-Hugues, R. Modelo matemático para la determinación del transporte longitudinal para playas del Caribe. *Tecnol. Cienc. Agua* **2011**, *II*, 127–140.
34. Hallermeier, R.J. A profilezonationforseasonalsandbeachesfrom wave climate. *Coast. Eng.* **1981**, *4*, 253–277. [\[CrossRef\]](#)
35. Peña Olivás, J.M.; Sánchez Palomar, F.J. Diques exentos: Inventario y comportamiento en las costas españolas. *Rev. Ing. Civil.* **2008**, *149*, 65–76.
36. Boak, E.H.; Turner, I.L. Shoreline Definition and Detection: A Review. *J. Coast. Res.* **2005**, *21*, 688–703. [\[CrossRef\]](#)
37. Fernández, M.; Díaz, P.; Ojeda, J.; Prieto, A.; Sánchez, N. Multipurpose line for mapping coastal information using a data model: The Andalusian coast (Spain). *J. Coast. Conserv.* **2015**, *19*, 461–474. [\[CrossRef\]](#)
38. Bartoletti, L. QGIS Python Plugin: Station Lines. Available online: <https://plugins.qgis.org/plugins/stationlines/,2014,consulta7.11.2019> (accessed on 11 July 2019).
39. Thieler, E.R.; Himmelstoss, E.A.; Zichichi, J.L.; Ergul, A. *Digital Shoreline Analysis System (DSAS) Version 4.0: An ArcGis Extension for Calculating Shoreline Changes*; Open-file Report; U.S. Geological Survey: Reston, VA, USA, 2009.
40. Dolan, R.; Fenster, M.S.; Holme, S.J. Temporal analysis of shoreline recession and accretion. *J. Coast. Res.* **1991**, *7*, 723–744.
41. Genz, A.S.; Fletcher, C.H.; Dunn, R.A.; Frazer, L.N.; Rooney, J. The predictive accuracy of shoreline change rate methods and alongshore beach variation on Maui, Hawaii. *J. Coast. Res.* **2011**, *23*, 87–105. [\[CrossRef\]](#)
42. Cowart, L.; Walsh, J.P.; Corbett, D.R. Analyzing Estuarine Shoreline Change: A Case Study of Cedar Island, North Carolina. *J. Coast. Res.* **2010**, *26*, 817–830. [\[CrossRef\]](#)
43. Martín Prieto, J.A.; Roig Munar, F.X.; Rodríguez Perea, A.; Mir Gual, M.; Pons Buades, G.X.; Gelabert Ferrer, B. La erosión histórica de la playa de saRàpita (S. Mallorca). *Investig. Geográficas* **2016**, *66*, 135–154. [\[CrossRef\]](#)
44. Morton, R.A.; Speed, F.M. Evaluation of shorelines and legal boundaries controlled by water levels on sandy beaches. *J. Coast. Res.* **1998**, *14*, 1373–1384.
45. Coyne, M.A.; Fletcher, H.; Richmond, B.M. Mapping coastal erosion hazards in Hawaii: Observations and errors. *J. Coast. Res.* **1999**, *28*, 171–184. [\[CrossRef\]](#)
46. Semeoschenkova, V.; Newton, A. Overview of erosion and beach quality issues in three Southern European countries: Portugal, Spain and Italy. *Ocean. Coast. Manag.* **2015**, *118*, 12–21. [\[CrossRef\]](#)
47. Ballesteros, C.; Jiménez, J.A.; Valdemoro, H.I.; Bosom, E. Erosion consequences on beach functions along the Maresme coast (NW Mediterranean, Spain). *Nat. Hazards* **2018**, *90*, 173–195. [\[CrossRef\]](#)
48. Molina, R.; Manno, G.; Re, C.L.; Anfuso, G.; Ciruolo, G. A Methodological Approach to Determine Sound Response Modalities to Coastal Erosion Processes in Mediterranean Andalusia (Spain). *J. Mar. Sci. Eng.* **2020**, *8*, 154. [\[CrossRef\]](#)
49. Ibarra Marinas, A.D. Análisis y evolución de las playas de la Región de Murcia (1956–2013). Ph.D. Thesis, Universidad de Murcia, Murcia, Spain, 2016; p. 351.
50. Lechuga Álvaro, A. Riesgos asociados al oleaje en zonas costeras. In *Riesgos Naturales*; Ayala Carcedo, F.J., Olcina Cantos, J., Eds.; Ariel Ciencia: Barcelona, Spain, 2002; pp. 1089–1098.



51. Landlin, M.C.; Patin, T.R.; Davies, J.E.; Palermo, M.R.; Clarke, D.G. Environmental Restoration and Habitat Development using Dredged Material in US Waters. In *Proceedings of the 14th World Dredging Congress—Dredging Benefits*, WODA; Central Dredging Association: Delft, The Netherlands, 1995.
52. Marbà, N.; Jordà, G.; Agustí, S.; Girard, C.; Duarte, C.M. Footprints of climate change on Mediterranean Sea biota. *Front. Mar. Sci.* **2015**, *2*, 1–11. [[CrossRef](#)]
53. Tigny, V.; Ozer, A.; De Falco, G.; Baroli, M.; Djenidi, S. Relationship between the Evolution of the Shoreline and the Posidonia oceanica Meadow Limit in a Sardinian Coastal Zone. *J. Coast. Res.* **2007**, *233*, 787–793. [[CrossRef](#)]
54. Ballesteros Pelegrín, G.A.; Fernández, J.; Belmonte, F.; Ibarra, D. Proyecto para la conservación de los hábitats y de las aves acuáticas en el LIC y ZEPA Salinas y Arenales de San Pedro del Pinatar (LIFE-SALINAS). In *Conservación, Gestión y Restauración de la Biodiversidad, Proceedings of the XI Congreso Español y I Congreso Iberoamericano de Biogeografía, Santander, Spain, 22–25 June 2020*; Carracedo, V., García-Codron, J.C., Garmendia, C., Rivas, V., Eds.; Asociación de Geógrafos Españoles (AGE): Santander, Spain, 2020; pp. 235–244.
55. Alonso Sarriá, F.; Gomariz Castillo, F.; Cánovas García, F. Conocimiento abierto en sistemas de información geográfica. Una estrategia para la geografía física. *Ninbus* **2012**, *29–30*, 21–31.
56. Dolan, R.; Hayden, B.P.; May, P.; May, S.K. The reliability of shoreline change measurements from aerial photographs. *Shore Beach* **1980**, *48*, 22–29. [[CrossRef](#)]
57. Shoshany, M.; Degani, A. Shoreline detection by digital image processing of aerial photography. *J. Coast. Res.* **1992**, *8*, 29–34.
58. Moore, L.J. Shoreline Mapping Techniques. *J. Coast. Res.* **2000**, *16*, 111–124.
59. Guariglia, A.; Buonomassa, A.; Losurdo, A.; Saladino, R.; Trivigno, M.L.; Zaccagnino, A.A. Multiource approach for coastline mapping and identification of shoreline changes. *Ann. Geophys.* **2006**, *49*, 295–304. [[CrossRef](#)]
60. Del Río, L.; Gracia, F.J. Error determination in the photogrammetric assessment of shoreline changes. *Nat. Hazards* **2013**, *63*, 2385–2397. [[CrossRef](#)]
61. Quartel, S.; Kroon, A.; Ruessink, B.G. Seasonal accretion and erosion patterns of a microtidal sandy beach. *Mar. Geol.* **2008**, *250*, 19–33. [[CrossRef](#)]